

CH6824025, Potent and Selective Discoidin Domain Receptor 1 Inhibitor, Reduces Kidney Fibrosis in Unilateral Ureteral Obstruction Mice[□]

Yukari Yasui, Takeshi Murata, Yoshinori Tsuboi,  Atsuko Murai, and  Naoshi Horiba

Research Division (Y.Y., T.M., Y.T., N.H.) and Translational Research Division (A.M.), Chugai Pharmaceutical Co., Ltd., Yokohama City, Kanagawa, Japan

Received May 30, 2024; accepted September 25, 2024

ABSTRACT

Discoidin domain receptor 1 (DDR1) is a collagen receptor with tyrosine kinase activity, and its expression is enhanced in various disease conditions. Although previous research suggests that DDR1 contributes to renal disease progression, DDR1 inhibitors for renal fibrosis have yet to be developed. In this study, we used unilateral ureteral obstruction (UUO) mice to investigate whether CH6824025, a strong and selective DDR1 phosphorylation inhibitor, can improve renal fibrosis. Furthermore, we performed 10x Visium spatial transcriptomics (ST) analysis on the kidney. CH6824025 suppressed the phosphorylation of DDR1 in the kidney, and the amount of hydroxyproline, the Sirius red- and the F4/80-positive area, and the mRNA expression of fibrosis and inflammation-related genes in the kidney were significantly decreased. 10x Visium ST analysis suggested that DDR1 is mainly expressed in distal nephrons under normal conditions but its expression appears to increase in the injured proximal tubules in UUO mice. Comparing mRNA expression in DDR1-positive spots in the Vehicle and the CH6824025 group, oxidative

phosphorylation and mitochondrial dysfunction might be improved, and pathways involved in fibrosis tended to be inhibited in the CH6824025 administration group. Downstream analysis would suggest that mRNA expression changes in the CH6824025 group contribute to the inhibition of cell movement. Taken together, our findings suggest that CH6824025 inhibited kidney fibrosis in UUO mice, which might be due to the inhibition of the migration of inflammatory cells to the injury site and the reduction of inflammation. DDR1 inhibitors are expected to be a promising treatment of renal fibrosis.

SIGNIFICANCE STATEMENT

The novel discoidin domain receptor 1 inhibitor CH6824025 could ameliorate fibrosis and inflammation in unilateral ureteral obstruction (UUO) mice. CH6824025 would inhibit cell motility (e.g., migration) that prevents the progression of fibrosis and improves mitochondrial function in UUO mice. CH6824025 could provide a significant benefit to patients with kidney fibrosis.

Introduction

The estimated prevalence of chronic kidney disease (CKD) worldwide was 9.1%, and the estimated number of deaths due to CKD reached 1.2 million. Furthermore, the prevalence has increased by approximately 30% since 1990, making CKD a disease with high medical needs (GBD Chronic Kidney Disease Collaboration, 2020). Although there have been remarkable advances in kidney transplantation and reno-protective medicine in recent years, there is a continued global demand to clarify the causes of CKD and develop drugs with renal protective effects.

Fibrosis in CKD correlates with renal function decline and can be a predictive marker for end-stage renal failure (Rodríguez-Iturbe et al., 2005). Various drugs, such as renin-angiotensin-aldosterone inhibitors, SGLT2 inhibitors, and mineral corticoid receptor inhibitors have been introduced in the past 20 years for the treatment of CKD. They have been successful in slowing the decline in renal function and extending the period until dialysis (Tang et al., 2022). These drugs are thought to suppress renal function decline through various mechanisms (e.g., renal parenchymal cell protection and the reduction of glomerular overload through tubular-glomerular feedback), in addition to the mechanisms initially assumed. However, no drug targeting kidney fibrosis has reached the market, and there is hope for the development of antifibrotic agents that can further suppress renal function decline when used in combination with existing drugs.

Discoidin domain receptor 1 (DDR1) is a collagen receptor with tyrosine kinase activity and is mainly expressed in

Primary laboratory of origin: Chugai Pharmaceutical Co., Ltd.

No author has an actual or perceived conflict of interest with the contents of this article.

[dx.doi.org/10.1124/jpet.124.002330](https://doi.org/10.1124/jpet.124.002330).

[□] This article has supplemental material available at jpet.aspetjournals.org.

ABBREVIATIONS: α SMA, α -smooth muscle actin; CD-PC, principal cells of collecting ducts; CKD, chronic kidney disease; CNT, connecting tubule; COL1A1, collagen type 1 α 1; COL3A1, collagen type 3 α 1; DDR1, discoidin domain receptor 1; IC-A, type A intercalated cells of collecting ducts; IC-B, type B intercalated cells of collecting ducts; PCR, polymerase chain reaction; PD, pharmacodynamics; PK, pharmacokinetics; PT, proximal tubules; ST, spatial transcriptomics; TGF, transforming growth factor; UUO, unilateral ureteral obstruction.

epithelial cells, playing a role in organ formation and maintenance of tissue homeostasis (Shrivastava et al., 1997; Vogel et al., 1997). DDR1 is also known to increase its expression and phosphorylation in various disease conditions such as fibrosis and cancer, and research on its relationship with disease progression, along with drug development, is actively being conducted (Borza and Pozzi, 2014; Moll et al., 2019; Tian et al., 2023). Although it has been reported that collagen binding to DDR1 induces autophosphorylation, which affects various cell functions such as adhesion, proliferation, and migration, the detailed molecular mechanism of how it affects cell functions in each cell remains unknown (Vogel et al., 2006; Leitinger, 2014; Dagamajalu et al., 2022). However, several findings suggesting the importance of DDR1 in renal disease have been obtained through research using DDR1 knockout mice. It has been variously reported that the deletion of DDR1 alleviates disease conditions in models such as Angiotensin-II load-induced hypertensive renal sclerosis, unilateral ureteral obstruction (UO), and Alport mice (Vogel et al., 2001; Flamant et al., 2006; Gross et al., 2010; Guerrot et al., 2011).

DDR1 shows high expression in non-small cell lung carcinoma, ovarian cancer, glioblastoma, and breast cancer, and is assumed to contribute to cancer progression, so DDR1 inhibitors have been actively researched mainly in the field of anti-cancer drug development (Elkamhawy et al., 2021). However, although low molecular weight compounds with high activity against DDR1 have been reported (Jeffries et al., 2020), they have not yet led to any clinical trials.

We developed CH6824025, which has strong and selective DDR1 phosphorylation inhibitory activity in vitro (Murata et al., 2013a, 2013b). Recently, we reported that DDR1 inhibitors suppress the activation of glomerular parietal epithelial cells and show renal protective effects in the NEP25 mouse model, which presents with focal segmental glomerular sclerosis-like glomerular epithelial cell injury (Moll et al., 2018). The NEP25 mouse model exhibits proteinuria-induced tubular injury and renal dysfunction due to prominent podocyte injury. Because DDR1 mainly expresses in epithelial cells, CH6824025 is thought to have protected the glomerular epithelial cells and tubules. In the same model, tubulointerstitial fibrosis was also suppressed, but it is unclear whether this suppression was secondary to the improvement in renal function or not. In this study, we conducted a pharmacological evaluation of CH6824025 using UO mice to examine its effect as a DDR1 inhibitor on fibrosis. Furthermore, to elucidate the mechanism of CH6824025 in more detail, we performed 10x Visium spatial transcriptomics (ST) analysis on the kidney.

Materials and Method

Chemicals. CH6824025 [3-chloro-*N*-[(5-chloro-2-ethylsulfonylphenyl)methyl]-4-[[3-(3-methylamino)piperidin-1-yl]methyl]-5-(trifluoromethyl)benzamide] (Fig. 1A) was synthesized by Chugai Pharmaceutical Co., Ltd. Details of synthesis are indicated in WO2013161851 (Example 200, Compound No. D-26) (Murata et al., 2013b).

In Vitro Experimental Design. U2OS cells stably expressing human DDR1 (gene ID: NM_013993) were seeded at 0.8×10^5 cells/well in a BioCoat Collagen I 96-well plate. Cells were preincubated with various concentrations of CH6824025 for 40 minutes at 37°C. Then, they were stimulated by adding

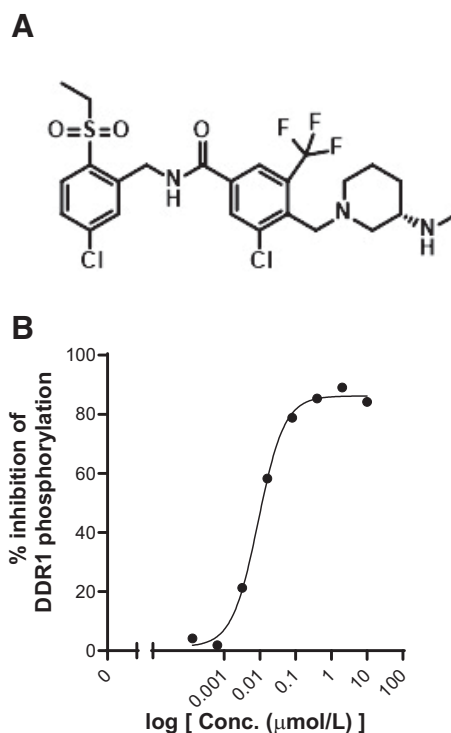


Fig. 1. Chemical structure and in vitro activity of CH6824025 on DDR1 phosphorylation. (A) Chemical structure of CH6824025. (B) Concentration-dependent inhibition of DDR1 phosphorylation by CH6824025 in U2OS cells. Each dot represents the mean of triplicate measurement.

type 1 collagen (final concentration 100 μg/ml) and incubated for over 16 hours at 37°C. After incubation, cells were lysed by the lysis buffer, which included Halt Protease & Phosphatase Inhibitor Single-Use Cocktail (Thermo Fisher Scientific Inc., Tokyo, Japan). The phosphorylation level of DDR1 was measured according to the protocol of DuoSet IC Human Phospho-DDR1 ELISA (R&D Systems Inc., Minneapolis, MN).

Animal Experiments. Male C57BL/6 J or ICR (Crlj;CD-1) were purchased from the Jackson Laboratories Japan, Inc. (Tokyo, Japan). Animal procedures and protocols were in accordance with the guidelines for the care and use of laboratory animals at Chugai Pharmaceutical Co. Ltd. and approved by the Institutional Animal Care and Use Committee (approval no. 11-239, 22-217, 23-117). Under isoflurane anesthesia, the abdomen was opened, and the left renal ureter was ligated to create a UO model. In the sham-operated animals (sham mice), a laparotomy was performed without ureteral ligation. Mice were fed on chow (CE-2; CLEA Japan Inc., Tokyo, Japan) ad libitum. Pharmacokinetics (PK) and pharmacodynamics (PD) studies were conducted using mice 6 or 7 days after UO surgery. In the PK study, UO mice were administered CH6824025 50 or 200 mg/kg ($n = 4$) and blood was collected at 4 or 24 hours after administration. The plasma concentration of CH6824025 was measured by liquid chromatography-tandem mass spectrometer (Waters Corporation, Milford, MA). In the PD study, sham or UO mice were administered vehicle or CH6824025 and killed at 24 hours after administration ($n = 3$). Kidneys were subjected to the analysis of DDR1 and phosphorylated DDR1 amount. In the first pharmacological study, mice were allocated to normal control ($n = 3$), disease control, or CH6824025-treated groups ($n = 10$, respectively) based on body weight 1 day before surgery. In the second pharmacological study for 10x

Visium ST analysis, mice were allocated to normal control ($n = 2$), disease control, or CH6824025-treated groups ($n = 5$, respectively) based on body weight 1 day before surgery. After the allocation, the oral once daily administration of vehicle or CH6824025 was started. Seven days after the treatment, mice were subjected to analysis.

Blood samples were collected from the abdominal portion of the vena cava under isoflurane anesthesia, and plasma samples were obtained by centrifugation. Kidneys were dissected for pathological analysis, and for the quantification of hydroxyproline amount and mRNA expression analysis.

Western Blotting Using Jess. The frozen kidneys were lysed in cell lysis buffer (Cell Signaling Technology Inc., Danvers, MA) with added protease and phosphatase inhibitor (Nacalai Tesque, Inc., Kyoto, Japan). Western blotting was performed using the simple western system Jess with a 12-230 kDa Separation Module (Bio-Techne Corp., Minneapolis, MN) according to manufacturer's instruction. Primary antibodies were purchased from Cell Signaling Technology Inc. and used in 1:250 dilution. Goat anti-rabbit secondary HRP conjugate (ready-to-use reagent) for Jess was used. The peak area was quantified using Compass software (Bio-Techne Corp.).

Pathological Analysis. The kidneys were fixed with 10% neutral buffered formalin solution and then embedded in paraffin. The paraffin blocks were cut and stained with H&E, Sirius red, and F4/80. The digital images of H&E staining were used for analysis. Five random cortical areas of the Sirius red or F4/80 specimen were selected, and the proportion of Sirius red or F4/80-positive areas was evaluated using Positive Pixel Count v9 in Aperio ImageScope v12.4.0.7018 (Leica Biosystems, GmbH, Wetzlar Germany). Using a deep learning tissue classification model with DenseNet AI V2 of HALO AI v3.4 (Indica laboratories, Albuquerque, NM), we annotated the tubular dilatation area in the cortex of the UUO kidneys. The classification model was created by a certified pathologist and confirmed by certified pathologists.

Measurement of Hydroxyproline Amount. The frozen kidneys were dried on a heat block at 120°C. The following day, the tissue weight was measured, 6 N HCl was added, and kidneys were heated again at 120°C. The following day, the remaining liquid was transferred to a 0.45 μ m filter plate and centrifuged. The hydroxyproline concentration was measured using liquid chromatography-tandem mass spectrometer (ACQUITY UPLC system) (Waters Corporation) coupled to an API 4000 triple quadrupole mass spectrometer system (Applied Biosystems/MDS SCIEX, MA).

Gene Expression Analysis. Total RNA was purified from the frozen kidneys using the RNeasy MINI kit (QIAGEN, Hilden, Germany), and the total RNA concentration was measured using NanoDrop 2000 (Thermo Fisher Scientific Inc.). PrimeTime qPCR Assays (IDT, Coralville, IA) or TaqMan gene expression assays (Thermo Fisher Scientific Inc.) were mixed with the purified total RNA, and quantitative real-time polymerase chain reaction (PCR) was performed using the 7900HT or QuantStudio5 Real-Time PCR System (Thermo Fisher Scientific Inc.). Expression levels are given as ratios to Mrpl19.

10x Visium ST Analysis and Pathway Analysis. Formalin-fixed, paraffin-embedded blocks of kidneys from each group (sham, $n = 1$; UUO vehicle group, $n = 3$; UUO CH6824025 200 mg/kg group, $n = 4$) in the second pharmacological study were selected, and 10x Visium ST analysis was

performed using Visium Spatial Gene Expression Reagent Kits for formalin-fixed, paraffin-embedded (10x Genomics, Inc., Pleasanton, CA) according to the manufacturer's instructions. Using Loupe Browser 6.5.0 (10x Genomics, Inc.), spots where the expression level of DDR1 was LogNorm >1 were extracted, and a gene expression list was created. The Log2FC and P -value of each gene for the UUO mice treated with vehicle compared with UUO mice treated with CH6824025 were calculated using Microsoft Excel for Microsoft 365 MSO 64 bit (Microsoft Corporation, Redmond, WA), and data were analyzed with the use of QIAGEN IPA (QIAGEN Inc., <https://digitalinsights.qiagen.com/IPA>) (Krämer et al., 2013).

Statistical Analysis. The calculation of each relative mRNA expression was performed using Microsoft Excel for Microsoft 365 MSO 64-bit (Microsoft Corporation). IC₅₀ calculation, and statistical analysis were performed using GraphPad Prism version 10.1.2 (GraphPad Software, Inc., Boston, MA). The nonlinear regression analysis was performed to calculate in vitro 50% inhibitory concentration. A comparison was made between the UUO vehicle group and sham or CH6824025 group using one-way ANOVA with posthoc Dunnett's multiple comparisons test.

Results

DDR1 Phosphorylation Inhibitory Activity of CH6824025. CH6824025 is highly selective, because the 451 types of kinases evaluated by KINOMEScan, only DDR1, DDR2, and lymphocyte-oriented kinase showed more than 99% competitive binding inhibition at 1 μ mol/l. (Moll et al., 2018). CH6824025 dose-dependently inhibited the phosphorylation of DDR1 induced by adding type 1 collagen to U2OS cells stably expressing DDR1, with an IC₅₀ of 8.9 nmol/l (Fig. 1B).

PK and PD Evaluation in UUO Mice. To determine the dosage for the efficacy evaluation test using the UUO mouse model, CH6824025 was orally administered at 50 or 200 mg/kg as a single dose to UUO mice on the day 6 or day 7 after surgery, and PK and PD were evaluated. Plasma concentrations of CH6824025 were maintained at 145 \pm 24 or 3540 \pm 410 ng/ml at 24 hours after administration in the 50 and 200 mg/kg administration groups, respectively (Table 1). Considering that the protein binding rate of CH6824025 in mouse blood is 1.1% (data not shown), the free concentration in the 200 mg/kg administration group was estimated to be approximately 70 nmol/l, which could mostly inhibit DDR1 phosphorylation in vitro. Next, we evaluated whether CH6824025 inhibits the phosphorylation of DDR1 in kidney tissue. In UUO mice, the protein levels of DDR1 and phosphorylated DDR1 significantly increased compared with sham (Fig. 2). CH6824025 dose-dependently decreased the phosphorylation of DDR1 at 50 or 200 mg/kg. Although a decrease in phosphorylation was observed in the 50 mg/kg administration group, the 200 mg/kg administration group showed a stronger DDR1 phosphorylation inhibitory effect. Based on the results of the PK and PD study, 200 mg/kg was selected as the administration dose for the following efficacy study.

The Effect of CH6824025 on Kidney Fibrosis and Inflammation in UUO Mice. On measuring DDR1 mRNA and protein in the kidney 7 days after UUO surgery, it was found that DDR1 mRNA and protein expression significantly increased in UUO mice compared with sham mice (Fig. 2,

TABLE 1

Concentration of CH6824025 in plasma of individual animals at 4 and 24 h after administration

CH6824025	Time (h)	Concentration (ng/ml)				Mean	SD
50 mg/kg oral administration	4	4260	3900	4150	3720	4010	240
	24	164	168	126	123	145	24
200 mg/kg oral administration	4	8040	6060	6690	6630	6860	840
	24	3620	4060	3380	3100	3540	410

Supplemental Fig. 1). In addition, the phosphorylation of DDR1 was notably enhanced in the kidney of UUO mice (Fig. 2). To clarify the effect of CH6824025 on kidney fibrosis, the amount of hydroxyproline and the Sirius Red positive areas in the kidney tissue of the vehicle group and the CH6824025 200 mg/kg group were measured 7 days after UUO surgery. The amount of hydroxyproline in the renal tissue significantly increased in the UUO mice compared with sham mice ($3833 \pm$

139 vs. 8301 ± 272 $\mu\text{g/g}$ tissue, $P < 0.05$), and this increase was significantly suppressed by the CH6824025 200 mg/kg administration (6918 ± 209 $\mu\text{g/g}$ tissue) (Fig. 3A). The Sirius red positive areas significantly increased in UUO mice compared with Sham mice (15.4 ± 0.5 vs. $3.9 \pm 0.3\%$, $P < 0.05$), and significantly decreased in the CH6824025 200 mg/kg group ($13.4 \pm 0.7\%$) (Fig. 3B, D–F). Furthermore, the HE stained specimens showed a significant tubular dilation in the CH6824025

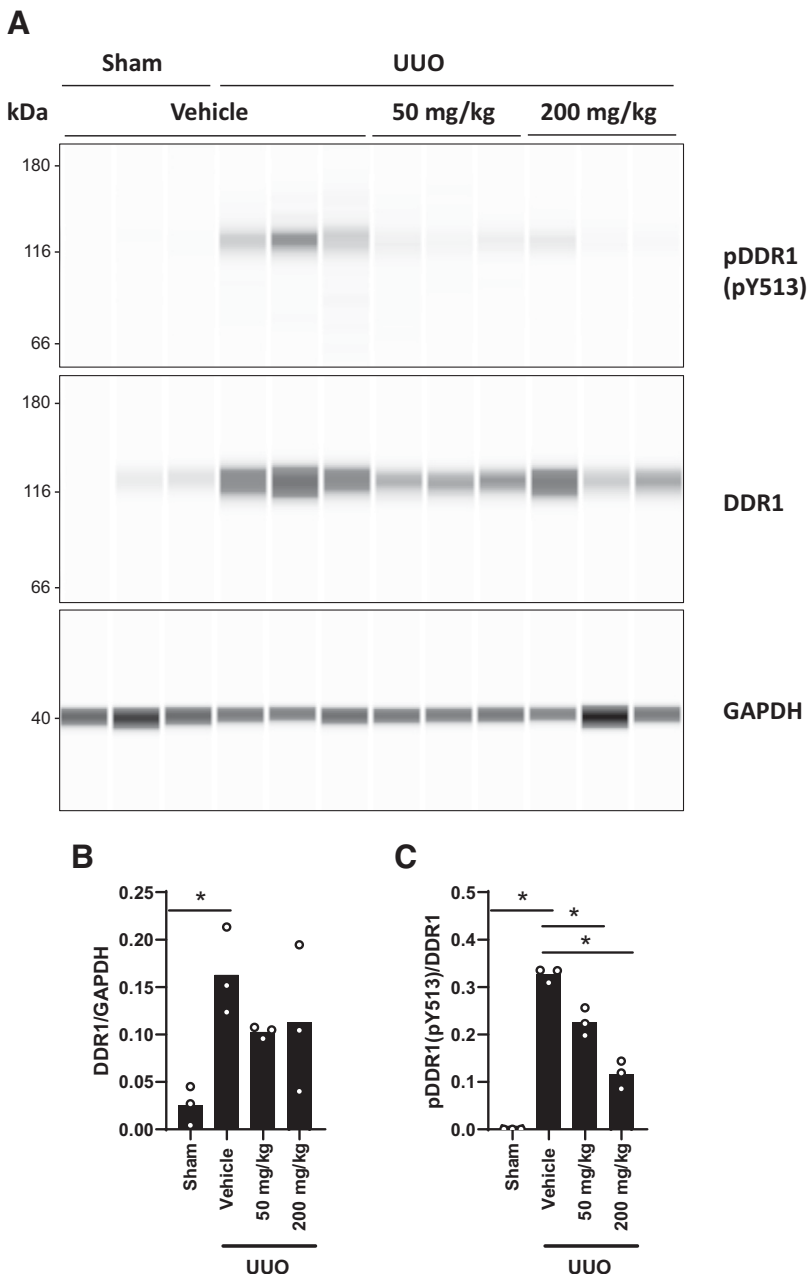


Fig. 2. PD evaluation of CH6824025 in UUO mice. (A) Western blotting of pDDR1(pY513), DDR1, and GAPDH in the kidney. The normalized peak area of (B) pDDR1(pY513) and (C) DDR1. The actual values are represented as dots and the columns represent mean ($n = 3$). * $P < 0.05$, significant difference versus UUO mice treated with vehicle (one-way ANOVA with posthoc Dunnett's multiple comparisons test). Sham: sham-operated mice. Vehicle: UUO mice treated with vehicle. 50 mg/kg or 200 mg/kg: UUO mice treated with CH6824025 50 mg/kg or 200 mg/kg.

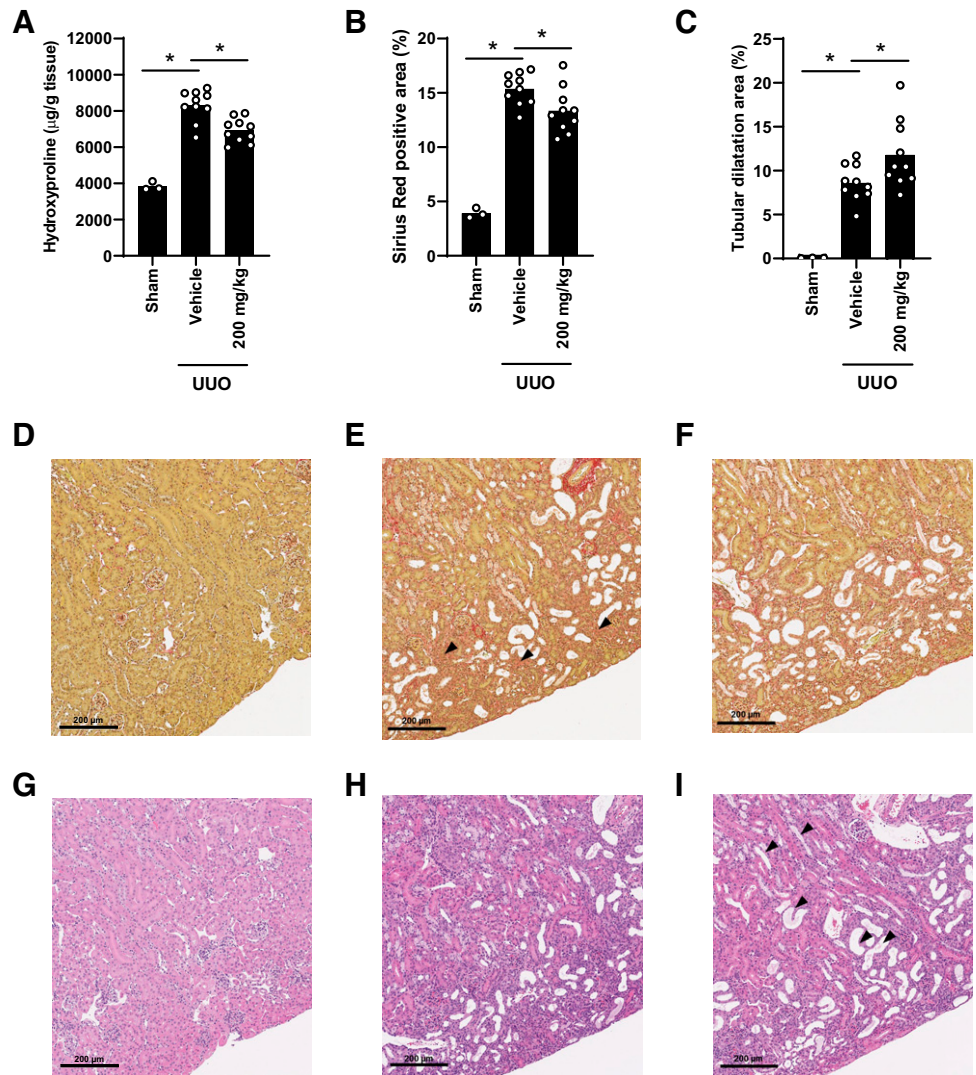


Fig. 3. Effect of CH6824025 on fibrosis in UUO mice. (A) Hydroxyproline amounts in the kidney. (B) Sirius Red positive area of kidney specimen. (C) The ratio of tubular dilatation in the kidney. The actual values are represented as dots, and the columns represent mean ($n = 3$ [sham], 10 [vehicle or 200 mg/kg]). * $P < 0.05$, significant difference versus UUO mice treated with vehicle (one-way ANOVA with posthoc Dunnett's multiple comparisons test). Sirius Red stained kidney of (D) sham mouse, (E) vehicle-treated UUO mouse, and (F) CH6824025 200 mg/kg-treated UUO mouse. Arrowheads indicate accumulation of collagen fibers. H&E stained kidney of (G) Sham mouse, (H) vehicle-treated UUO mouse, and (I) CH6824025 200 mg/kg-treated UUO mouse. Arrowheads indicate dilation of tubule. Sham: sham-operated mice. Vehicle: UUO mice treated with vehicle. 200 mg/kg: UUO mice treated with CH6824025 200 mg/kg.

200 mg/kg group compared with the vehicle group (11.8 ± 1.2 vs. $8.6 \pm 0.6\%$, $P < 0.05$) (Fig. 3C, G–I; Supplemental Fig. 2).

Given that fibrosis in UUO kidneys was suppressed by CH6824025 administration, the expression levels of fibrosis-related mRNA in renal tissue were evaluated by real-time quantitative PCR. The expression levels of each mRNA of COL1A1, COL3A1, α -SMA, transforming growth factor (TGF)- β 1, and TIMP2 increased in the UUO mice compared with sham mice, and these increases were significantly ameliorated by CH6824025 at 200 mg/kg (Fig. 4A–E). In addition, we measured the expression levels of inflammation-related genes and evaluated the immunohistochemistry of the F4/80 positive area to find the effect on the infiltration of inflammatory cells into the kidneys. The mRNA expression levels of CCL2, tumor necrosis factor- α , and CD3E increased in UUO mice compared with sham mice, and all of these levels were significantly decreased by CH6824025 at 200 mg/kg (Fig. 4F–H). The F4/80-positive areas significantly increased in UUO mice compared with sham mice (4.8 ± 0.7 vs. $1.6 \pm 0.2\%$, $P < 0.05$), and significantly decreased in the CH6824025 200 mg/kg group ($2.7 \pm 0.2\%$) (Fig. 5). These data suggested that CH6824025 decreased fibrosis and inflammation in UUO mice.

10x Visium ST Analysis and Pathway Analysis. To analyze the antifibrotic action of CH6824025 in detail, 10x Visium ST analysis was performed on the kidney. In sham mice, DDR1 was primarily expressed in the medulla and partly in the cortex (Fig. 6A). On the other hand, in UUO mice, DDR1 mRNA expression increased greatly in the inner medulla and cortex (Fig. 6B) and its expression was not changed by CH6824025 treatment (Fig. 6C). When using K-methods to cluster the regions where DDR1 is relatively highly expressed, they were classified into four different clusters in sham mice and UUO mice, respectively (Supplemental Fig. 3A–D). Compared with the expression of renal marker genes, the pattern of DDR1 expression was found to be similar to that of marker genes of the distal nephron, such as the connecting tubule (CNT), principal cells of collecting ducts (CD-PC), type A intercalated cells of collecting ducts (IC-A), and type B intercalated cells of collecting ducts (IC-B) (Supplemental Fig. 3A). On the other hand, they did not completely match the cluster with high expression of Lrp2, a proximal tubules (PT) marker (Supplemental Fig. 3B), and showed a tendency to match the expression distribution of DDR1 in normal mice, referenced from previously reported single-cell RNA-sequencing data

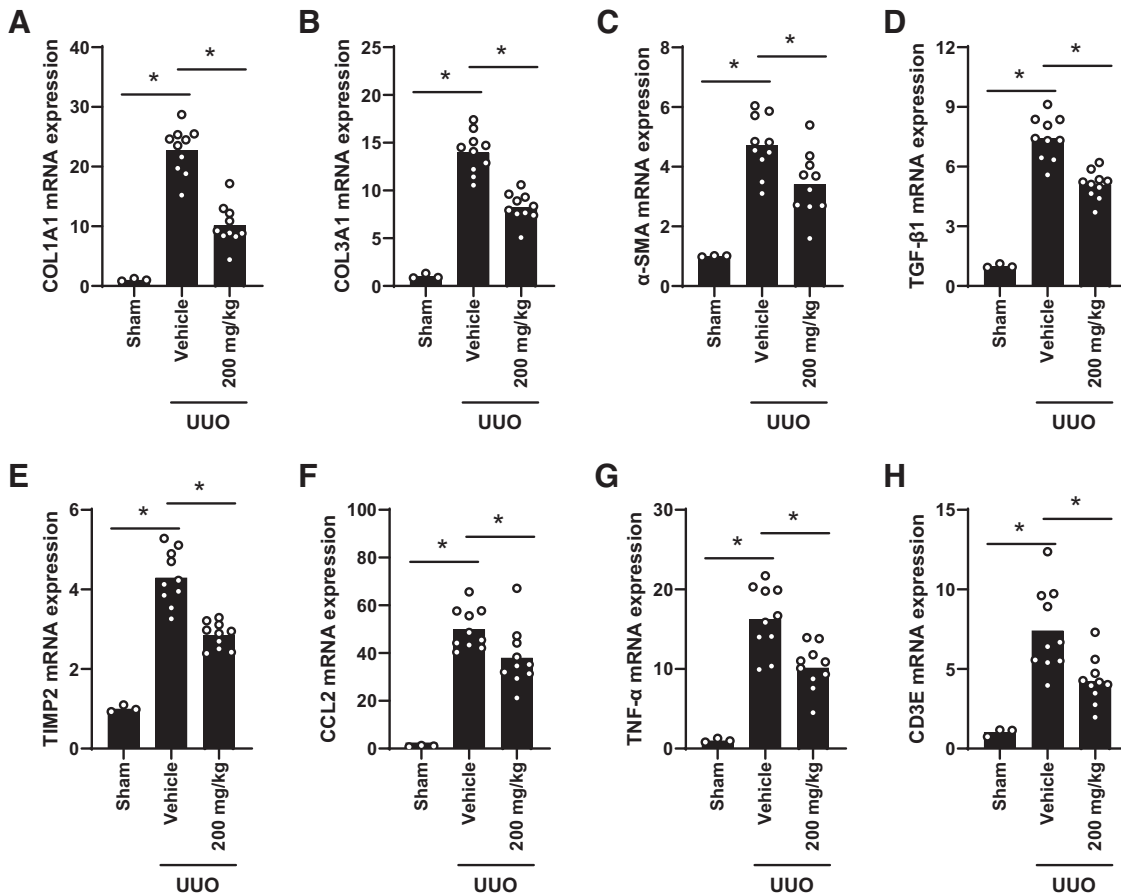


Fig. 4. Effect of CH6824025 on the mRNA expression of fibrotic and proinflammatory markers in UUO mice. Relative (A) COL1A1, (B) COL3A1, (C) α -SMA, (D) TGF- β 1, (E) TIMP2, (F) CCL2, (G) tumor necrosis factor- α , and (H) CD3E mRNA expression in the kidney. Expression levels are given as ratios to Mrpl19. The actual values are represented as dots, and the columns represent mean ($n = 3$ [sham], 10 [vehicle or 200 mg/kg]). * $P < 0.05$, significant difference versus UUO mice treated with vehicle (one-way ANOVA with posthoc Dunnett's multiple comparisons test). Sham: sham-operated mice. Vehicle: UUO mice treated with vehicle. 200 mg/kg: UUO mice treated with CH6824025 200 mg/kg.

(Kidney Interactive Transcriptomics; <https://humphreyslab.com/SingleCell/>) (Li et al., 2022). When examining the clusters with high DDR1 expression in UUO mice, the expression pattern of the DDR1 was found to match the pattern of expression of CNT and IC-B marker genes, similar to the sham mice (Supplemental Fig. 3C). On the other hand, in UUO mice, unlike sham mice, clusters with high expression of DDR1 and Lrp2 were observed (Supplemental Fig. 3D). In particular, cluster 1, indicated in blue, was suggested to be a cell population containing a large number of PTs, because Lrp2 and glomerular marker Nphs1 were relatively high, and the marker genes of each distal nephron from CNT to CD-PC were relatively low. Furthermore, it was found that among the clusters with high DDR1 expression in UUO mice, there were clusters with high expression of markers (e.g., Vcam1 and Havcr1) of injured PT and failed repair PT cells (clusters 1,4,7 in Supplemental Fig. 3E). Based on these results, DDR1 expressing spots ($\text{LogNorm} > 1$) in the kidneys of the UUO mice treated with vehicle or CH6824025 200 mg/kg were selected (Fig. 6D–F) and differentially expression genes analysis was performed. A total of 98 or 220 genes, which were upregulated or downregulated in UUO mice treated with CH6824025, were identified that had a P -value of 0.05 or less and $\text{Log}_2\text{FC} > |0.5|$ in the Student's t test. The top 50 genes with the largest expression

changes are shown in Supplemental Table 1. These groups of genes (98 and 220 genes) were used to perform canonical pathway analysis in Ingenuity pathway analysis. The CH6824025 200 mg/kg administration group showed inhibition of “mitochondrial dysfunction” and “pulmonary fibrosis idiopathic signaling pathway” and enhancement of “oxidative phosphorylation” (Fig. 7A). Further downstream analysis revealed significant inhibitory effects on the “cellular movement” category, including Ccl5, Ccr2, and Glipr2, in the CH6824025 200 mg/kg administration group (Fig. 7B).

Discussion

This study is the first to evaluate the antifibrotic effects of a newly created, highly active and selective oral DDR1 inhibitor, CH6824025, in kidney fibrosis. We found that CH6824025 had strong DDR1 phosphorylation inhibitory activity both in vitro and in vivo and that it ameliorated kidney fibrosis in UUO mice. Because DDR1 is expressed in different types of human glomerular nephritis (Moll et al., 2018), CH6824025 could potentially inhibit various types of renal fibrosis across different etiologies.

10x Visium ST analysis indicated that DDR1 mRNA is dominantly expressed in the same region of distal nephron marker

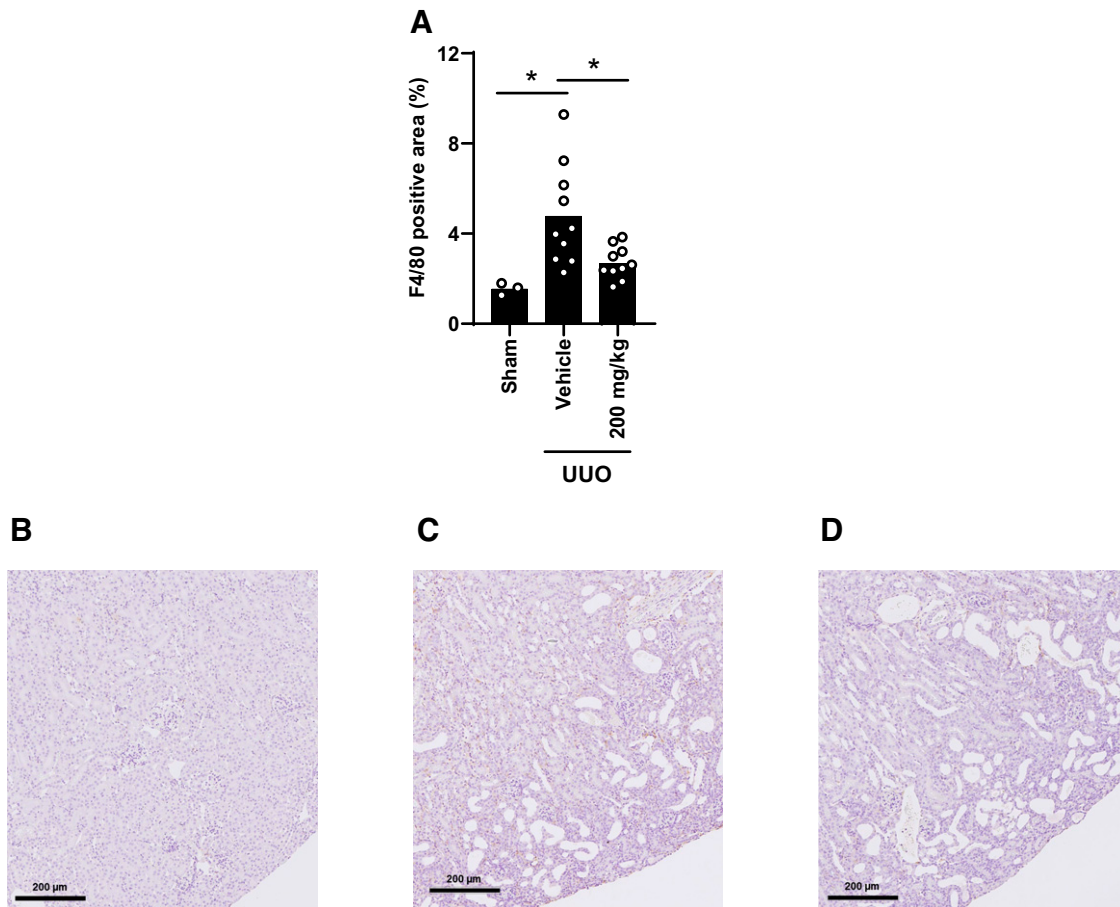


Fig. 5. Effect of CH6824025 on F4/80⁺ macrophages in UUO mice. (A) F4/80 positive area of kidney specimen. The actual values are represented as dots, and the columns represent mean ($n = 3$ [sham], 10 [vehicle or 200 mg/kg]). * $P < 0.05$, significant difference versus UUO mice treated with vehicle (one-way ANOVA with posthoc Dunnett's multiple comparisons test). F4/80-stained kidney of (B) sham mouse, (C) vehicle-treated UUO mouse, and (D) CH6824025 200 mg/kg-treated UUO mouse. Sham: sham-operated mice. Vehicle: UUO mice treated with vehicle. 200 mg/kg: UUO mice treated with CH6824025 200 mg/kg.

genes, namely CNT, IC-A, IC-B, and CD-PC in the normal mouse kidney. On the other hand, in the UUO mouse kidney, an increase of DDR1 mRNA expression in the injured PT was suggested. Furthermore, because DDR1 phosphorylation was enhanced in the kidney lysate of UUO mice, it is speculated that DDR1 expression and phosphorylation were enhanced in the injured cells of the UUO kidney.

In the CH6824025 administration group, the amount of hydroxyproline and the Sirius red positive area in the kidney tissue were significantly reduced. When the mRNA expression levels in the kidney tissue were evaluated by quantitative real-time PCR, the expression of fibrosis and inflammation-related molecules was significantly reduced by the administration of CH6824025. In DDR1 null mice, the infiltration of F4/80⁺ macrophages and Cd3⁺ T cells into the UUO kidney is reported to be suppressed and the expression levels of inflammatory cytokines and chemokines reduced (Guerrot et al., 2011). Moreover, the administration of CH6824025 tended to suppress the expression of COL4A1 and TGF- β 1 in the analysis with 10x Visium ST. It has been reported that the stimulation of collagen 1 induces the nuclear translocation of DDR1, which suppresses the expression of COL4A1 (Chiusa et al., 2019). Additionally, DDR1 has been reported to suppress the expression of TGF- β 1 by controlling the phosphorylation of the breakpoint cluster region and STAT3 (Borza et al., 2022).

The antifibrotic effect of CH6824025 observed in this study may have occurred in part due to the inhibition of the nuclear translocation of DDR1, as well as the phosphorylation of breakpoint cluster region and STAT3.

We used the kidney tissue collected on day 7 after the UUO operation to perform 10x Visium ST to analyze the mechanism underlying CH6824025's antifibrotic effect. Our finding in this study that DDR1 mRNA appeared to be expressed in the injured PT of UUO mice is consistent with a previous study (Moll et al., 2018), which demonstrated the localization of DDR1 in the PT in systemic lupus erythematosus patients.

When we analyzed the changes in gene expression in DDR1-positive spots in the UUO vehicle group and the CH6824025 group, CH6824025 either increased or decreased the expression of 98 or 220 genes. A subsequent analysis using the IPA pathway analysis suggested the inhibition of mitochondrial dysfunction, suppression of pulmonary fibrosis idiopathic signaling pathways, and an escalation in oxidative phosphorylation. Further downstream analysis implied that cell migration was suppressed by the administration of CH6824025. Based on these analyses, we postulate that the administration of CH6824025 resulted in the inhibition of inflammatory cell activation, the mitigation of fibrosis, and improvements in both mitochondrial function and oxidative phosphorylation.

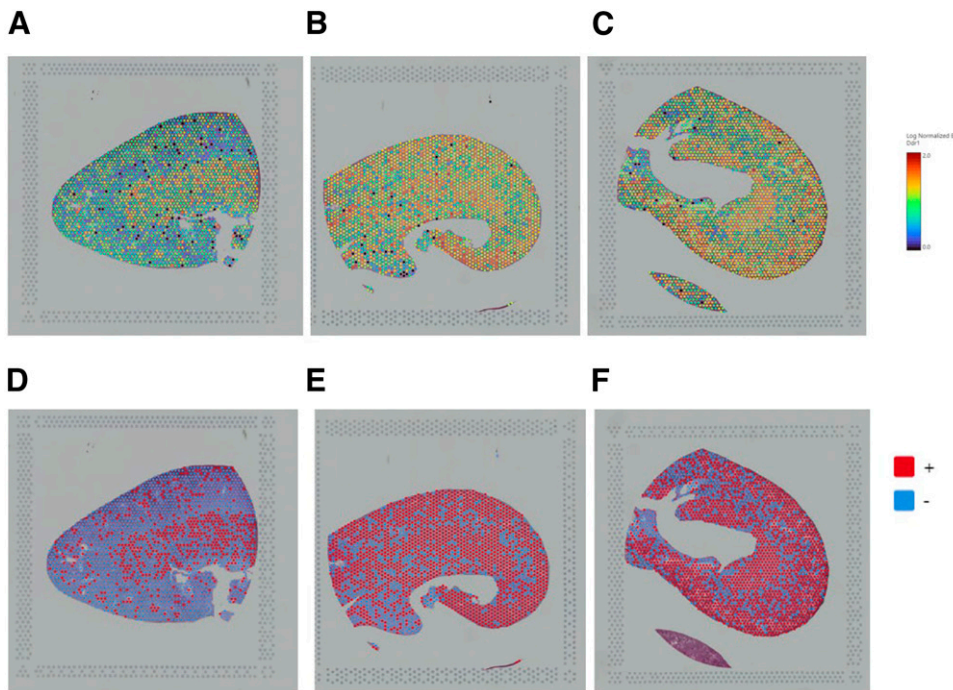


Fig. 6. 10x Visium ST analysis of UO mouse kidneys treated with CH6824025. DDR1 mRNA expression in the kidney of (A) sham mouse, (B) vehicle-treated UO mouse, and (C) CH6824025 200 mg/kg-treated UO mouse. Selected spots as DDR1 mRNA-positive spots in the kidney of (D) sham mouse, (E) vehicle-treated UO mouse, and (F) CH6824025 200 mg/kg-treated UO mouse. Red or blue spots indicate DDR1 positive or negative spots, respectively.

The gene with the highest increase in expression in the CH6824025 administration group was *Calb1*. *Calb1* is a marker gene for CNT, and colocalization with DDR1 is also observed in human normal kidney samples (Moll et al., 2018). It has been reported that the expression of *Calb1* decreases with distal nephron injury associated with UO and human IgA nephropathy (Iida et al., 2014). When we confirmed the localization of *Calb1* along with renal pathological changes using 10x Visium ST analysis, *Calb1* was mainly expressed in expanded renal tubules in the cortical region of the UO kidney. As mentioned, despite the greater tubular dilation in the CH6824025 group compared with the UO vehicle group, the fact that the expression of *Calb1* remained high in the CH6824025 administration group is intriguing, suggesting that the DDR1 inhibitor has a protective effect on CNT injury. In addition, we conducted a 4-day preliminary toxicity study using 200 mg/kg of CH6824025 and found no evidence of renal toxicity, including in serum creatinine and urea nitrogen levels, or histopathology.

In the CH6824025 group, there was a significant tubular expansion compared with the UO Vehicle group. We think this is caused by the reduced production of surrounding fibrous components, which made the tubular expansion due to pressure load more visible. Similar to CH6824025, it has been reported that in Biglycan null mice with UO, the tubules were greatly expanded compared with wild type mice with UO (Schaefer et al., 2004). In their study, evaluation continued up to 70 days after the creation of UO, so strong expansion was observed up to the Bowman's space. Our current evaluation of CH6824025 was only up to 7 days after the creation of UO. We think that if we administer CH6824025 for a longer period, it will be possible to clearly observe the expansion of the lumen due to the reduction of fibrous components.

Finally, we will mention the limitations of this study. First, we only evaluated the efficacy of CH6824025 against fibrosis in a preventive regimen. In chronic kidney disease, it is not

uncommon for fibrosis to have already progressed, so it is also important to show efficacy from a late stage. Furthermore, although CH6824025 has demonstrated a reno-protective effect in the NEP mouse model (Moll et al., 2018), it is necessary to verify whether CH6824025 has a reno-protective effect in progressive kidney disease models accompanied by renal fibrosis, such as the 5/6 nephrectomy model or the Alport mouse model.

Second, we only performed analysis using 10x Visium ST analysis alone, and it was difficult to annotate the cell types due to a resolution limit. Although 10x Visium ST analysis is a powerful tool for evaluating the relationship between renal morphological changes and gene expression levels, it is difficult to identify DDR1-expressing cells at a single-cell resolution because each spot contains approximately 10 cells. Our next challenge is to evaluate the mechanism of action of the drugs more precisely in target cells and to link this to pathological changes by integrating single-cell analysis and 10x Visium ST analysis or by using a new technology like Visium HD.

In summary, in this study, we showed that CH6824025, a selective DDR1 phosphorylation inhibitor, inhibited kidney fibrosis in UO mice, which might be due to the inhibition of the migration of inflammatory cells to the injury site and the reduction of inflammation. Furthermore, CH6824025 might ameliorate the impairment of mitochondrial function and exert robust antifibrotic effects. Although antihypertensive and immunosuppressive drugs can indirectly inhibit renal fibrosis by improving renal function, there are no approved drugs that directly inhibit renal fibrosis yet. This study revealed that CH6824025 could effectively inhibit renal fibrosis. Because DDR1-dependent fibrosis is clinically important from the perspective of its expression pattern (Moll et al., 2018), CH6824025 may be effective not only as monotherapy, but also in combination with drugs targeting mechanisms other than fibrosis. The novel DDR1 inhibitor CH6824025 is expected to be a promising treatment of renal fibrosis.

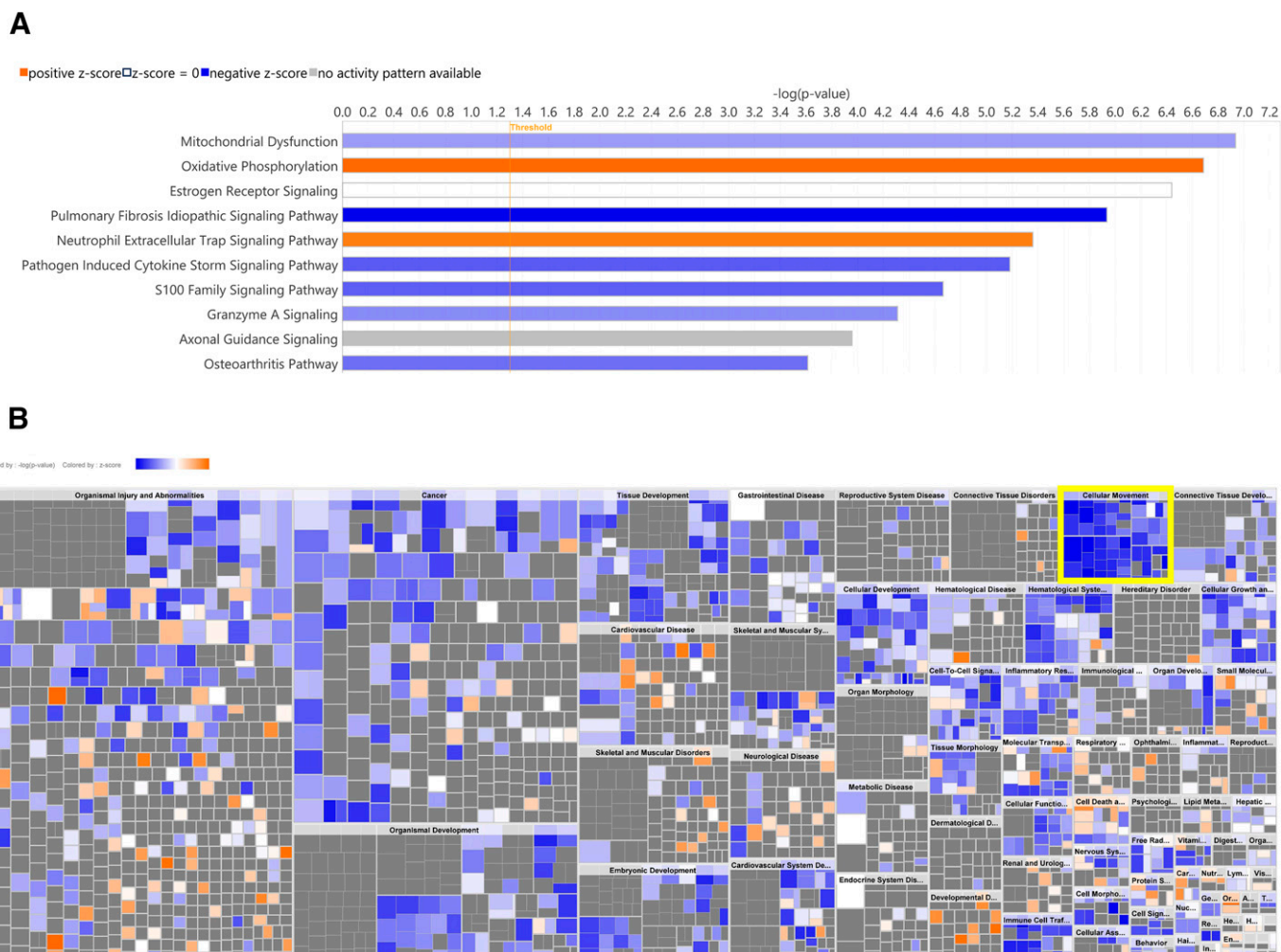


Fig. 7. Ingenuity pathway analysis of DDR1 positive spots in the kidney of UO mice treated with CH6824025. (A) Canonical pathway analysis that shows the results of the top 10 pathways. The bar chart is colored based on the z-score. (B) Analysis of disease and functions. The heatmap is colored based on the z-score. The color reflects the direction of change in the biological process. Orange color represents a trend to increase; blue represents a trend to decrease in UO mice treated with CH6824025 compared with Vehicle-treated UO mice. Gray indicates that no activity prediction can currently be made. White indicates (1) pathways with z-scores at or very close to 0; or (2) those that are ineligible for analysis because there are fewer than four analysis-ready molecules in the dataset associated with the pathway. The size of each rectangle indicates the *P*-value significance. The yellow rectangle highlights “cellular movement.”

Acknowledgments

The authors thank Perez Chieko, Mei Banba (Chugai Pharmaceutical Co., Ltd.), and Hidekazu Kitamura (Chugai Research Institute for Medical Science, Inc.) for their technical assistance and Jacob Davis (Chugai Pharmaceutical Co., Ltd.) for his assistance with English usage. This work received no external funding.

Data Availability

10x Visium ST analysis data are openly available in Gene Expression Omnibus (accession number: GSE273978). All other data presented are contained within the manuscript and/or the Supplemental Material.

Authorship Contributions

Participated in research design: Yasui, Horiba.
Conducted experiments: Yasui.
Contributed new reagents or analytic tools: Murata.
Performed data analysis: Yasui, Murai.
Wrote or contributed to the writing of the manuscript: Yasui, Tsuboi, Horiba.

References

- Borza CM, Bolas G, Bock F, Zhang X, Akabogu FC, Zhang M-Z, de Caestecker M, Yang M, Yang H, Lee E, et al. (2022) DDR1 contributes to kidney inflammation and fibrosis by promoting the phosphorylation of BCR and STAT3. *JCI Insight* 7:e150887.
- Borza CM and Pozzi A (2014) Discoidin domain receptors in disease. *Matrix Biol* 34:185–192.
- Chiusa M, Hu W, Liao H-J, Su Y, Borza CM, de Caestecker MP, Skrypnik NI, Fogo AB, Pedchenko V, Li X, et al. (2019) The extracellular matrix receptor discoidin domain receptor 1 regulates collagen transcription by translocating to the nucleus. *J Am Soc Nephrol* 30:1605–1624.
- Dagamajalu S, Rex DAB, Suchitha GP, Rai AB, Kumar S, Joshi S, Raju R, and Prasad TSK (2022) A network map of discoidin domain receptor 1(DDR1)-mediated signaling in pathological conditions. *J Cell Commun Signal* 17:1081–1088.
- Elkamdawy A, Lu Q, Nada H, Woo J, Quan G, and Lee K (2021) The journey of DDR1 and DDR2 kinase inhibitors as rising stars in the fight against cancer. *Int J Mol Sci* 22:6535.
- Flamant M, Placier S, Rodenas A, Curat CA, Vogel WF, Chatziantoniou C, and Dussaule J-C (2006) Discoidin domain receptor 1 null mice are protected against hypertension-induced renal disease. *J Am Soc Nephrol* 17:3374–3381.
- GBD Chronic Kidney Disease Collaboration. (2020) Global, regional, and national burden of chronic kidney disease, 1990–2017: a systematic analysis for the Global Burden of Disease Study 2017. *Lancet* 395:709–733.
- Gross O, Girgert R, Beirowski B, Kretzler M, Kang HG, Kruegel J, Miosge N, Busse A-C, Segerer S, Vogel WF, et al. (2010) Loss of collagen-receptor DDR1 delays renal fibrosis in hereditary type IV collagen disease. *Matrix Biol* 29:346–356.
- Guerrot D, Kerroch M, Placier S, Vandermeersch S, Trivin C, Mael-Ainin M, Chatziantoniou C, and Dussaule J-C (2011) Discoidin domain receptor 1 is a major

- mediator of inflammation and fibrosis in obstructive nephropathy. *Am J Pathol* **179**:83–91.
- Iida T, Fujinaka H, Xu B, Zhang Y, Magdeldin S, Nameta M, Liu Z, Yoshida Y, Yaoita E, Tomizawa S, et al. (2014) Decreased urinary calbindin 1 levels in proteinuric rats and humans with distal nephron segment injuries. *Clin Exp Nephrol* **18**:432–443.
- Jeffries DE, Borza CM, Blobaum AL, Pozzi A, and Lindsley CW (2020) Discovery of VU6015929: a selective discoidin domain receptor 1/2 (DDR1/2) inhibitor to explore the role of DDR1 in antifibrotic therapy. *ACS Med Chem Lett* **11**:29–33.
- Krämer A, Green J, Pollard J, and Tugendreich S (2013) Causal analysis approaches in ingenuity pathway analysis. *Bioinformatics* **30**:523–530.
- Leitinger B (2014) Discoidin domain receptor functions in physiological and pathological conditions. *Int Rev Cell Mol Biol* **310**:39–87.
- Li H, Dixon EE, Wu H, and Humphreys BD (2022) Comprehensive single-cell transcriptional profiling defines shared and unique epithelial injury responses during kidney fibrosis. *Cell Metab* **34**:1977–1998.e1979.
- Moll S, Desmoulière A, Moeller MJ, Pache J-C, Badi L, Arcadu F, Richter H, Satz A, Uhles S, Cavalli A, et al. (2019) DDR1 role in fibrosis and its pharmacological targeting. *Biochim Biophys Acta Mol Cell Res* **1866**:118474.
- Möll S, Yasui Y, Abed A, Murata T, Shimada H, Maeda A, Fukushima N, Kanamori M, Uhles S, Badi L, et al. (2018) Selective pharmacological inhibition of DDR1 prevents experimentally-induced glomerulonephritis in prevention and therapeutic regime. *J Transl Med* **16**:148.
- Murata T, Kawada H, Niizuma S, Hara S, Hada K, Shimada H, Tanaka H, and Mio T (2013a) inventors. Preparation of quinazolinone derivatives as discoidin domain receptor 1 (DDR1) inhibitors. US Patent WO2013/161853 A1. 2013 Oct 31.
- Murata T, Niizuma S, Hara S, Kawada H, Hada K, Shimada H, Tanaka H, and Nakanishi Y (2013b) inventors. Preparation of benzamide derivatives as discoidin domain receptor 1 (DDR1) inhibitors. US Patent WO2013/161851 A1. 2013 Oct 31.
- Rodríguez-Iturbe B, Johnson RJ, and Herrera-Acosta J (2005) Tubulointerstitial damage and progression of renal failure. *Kidney Int Suppl* **68**:S82–S86.
- Schaefer L, Mihalik D, Babelova A, Krzyzankova M, Gröne H-J, Iozzo RV, Young MF, Seidler DG, Lin G, Reinhardt DP, et al. (2004) Regulation of fibrillin-1 by biglycan and decorin is important for tissue preservation in the kidney during pressure-induced injury. *Am J Pathol* **165**:383–396.
- Shrivastava A, Radziejewski C, Campbell E, Kovac L, McGlynn M, Ryan TE, Davis S, Goldfarb MP, Glass DJ, Lemke G, et al. (1997) An orphan receptor tyrosine kinase family whose members serve as nonintegrin collagen receptors. *Mol Cell* **1**:25–34.
- Tang J, Liu F, Cooper ME, and Chai Z (2022) Renal fibrosis as a hallmark of diabetic kidney disease: potential role of targeting transforming growth factor-beta (TGF- β) and related molecules. *Expert Opin Ther Targets* **26**:721–738.
- Tian Y, Bai F, and Zhang D (2023) New target DDR1: a “double-edged sword” in solid tumors. *Biochim Biophys Acta Rev Cancer* **1878**:188829.
- Vogel W, Gish GD, Alves F, and Pawson T (1997) The discoidin domain receptor tyrosine kinases are activated by collagen. *Mol Cell* **1**:13–23.
- Vogel WF, Abdulhussein R, and Ford CE (2006) Sensing extracellular matrix: an update on discoidin domain receptor function. *Cell Signal* **18**:1108–1116.
- Vogel WF, Aszódi A, Alves F, and Pawson T (2001) Discoidin domain receptor 1 tyrosine kinase has an essential role in mammary gland development. *Mol Cell Biol* **21**:2906–2917.

Address correspondence to: Yukari Yasui, Chugai Life Science Park Yokohama, Chugai Pharmaceutical Co., Ltd., 216 Totsuka-cho, Totsuka-ku, Yokohama 244-860, Japan. E-mail: yasui.yukari16@chugai-pharm.co.jp

CH6824025, potent and selective DDR1 inhibitor, reduces kidney fibrosis in UUO mice

Names of authors

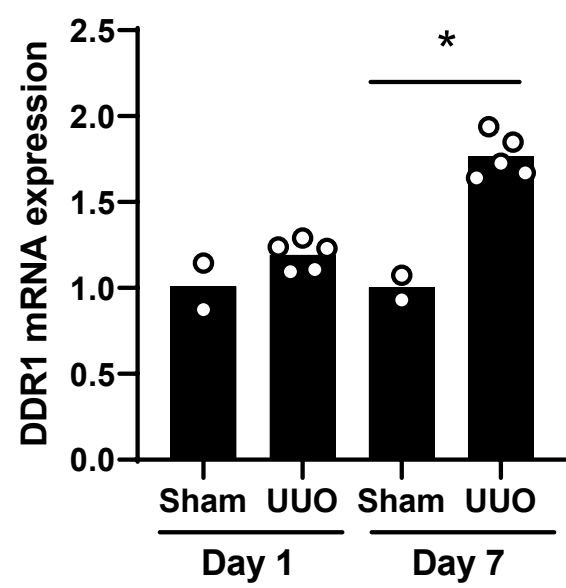
Yukari Yasui, Takeshi Murata, Yoshinori Tsuboi, Atsuko Murai, Naoshi Horiba

Research Division, Chugai Pharmaceutical Co., Ltd., Yokohama city, Kanagawa, Japan. (Y.Y., T.M., Y.T., N.H.)

Translational Research Division, Chugai Pharmaceutical Co., Ltd., Yokohama city, Kanagawa, Japan. (A.M.)

The Journal of Pharmacology and Experimental Therapeutics

JPET-AR-2024-002330



Supplemental Figure 1. Relative DDR1 mRNA expression in the kidney at day 1 and 7 after the surgery. The actual values are represented as dots, and the columns represent mean. n=2 (Sham), n=5 (Vehicle and 200 mg/kg). *P<0.05 significant difference versus UUO mice treated with vehicle (Student's t-test).

CH6824025, potent and selective DDR1 inhibitor, reduces kidney fibrosis in UUO mice

Names of authors

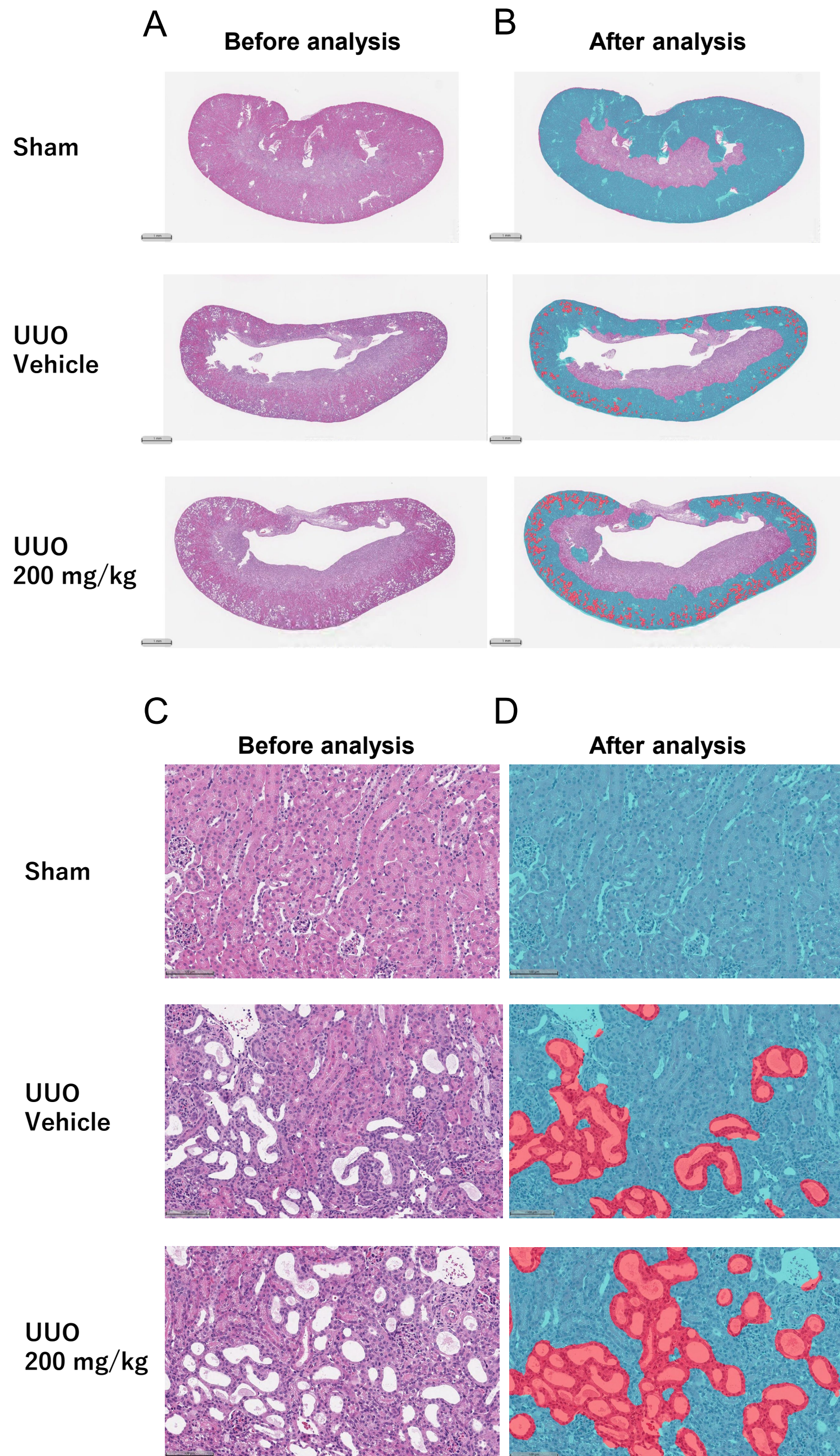
Yukari Yasui, Takeshi Murata, Yoshinori Tsuboi, Atsuko Murai, Naoshi Horiba

Research Division, Chugai Pharmaceutical Co., Ltd., Yokohama city, Kanagawa, Japan. (Y.Y., T.M., Y.T., N.H.)

Translational Research Division, Chugai Pharmaceutical Co., Ltd., Yokohama city, Kanagawa, Japan. (A.M.)

The Journal of Pharmacology and Experimental Therapeutics

JPET-AR-2024-002330



Supplemental Figure 2. Histopathological images (**A, C**) before and (**B, D**) after classification of HALO AI v3.4. Red, tubular dilatation area; light blue, kidney area except tubular dilatation area. HE staining. Bar, (**A, B**) 1 mm, or (**C, D**), 100 μ m.

CH6824025, potent and selective DDR1 inhibitor, reduces kidney fibrosis in UUO mice

Names of authors

Yukari Yasui, Takeshi Murata, Yoshinori Tsuboi, Atsuko Murai, Naoshi Horiba

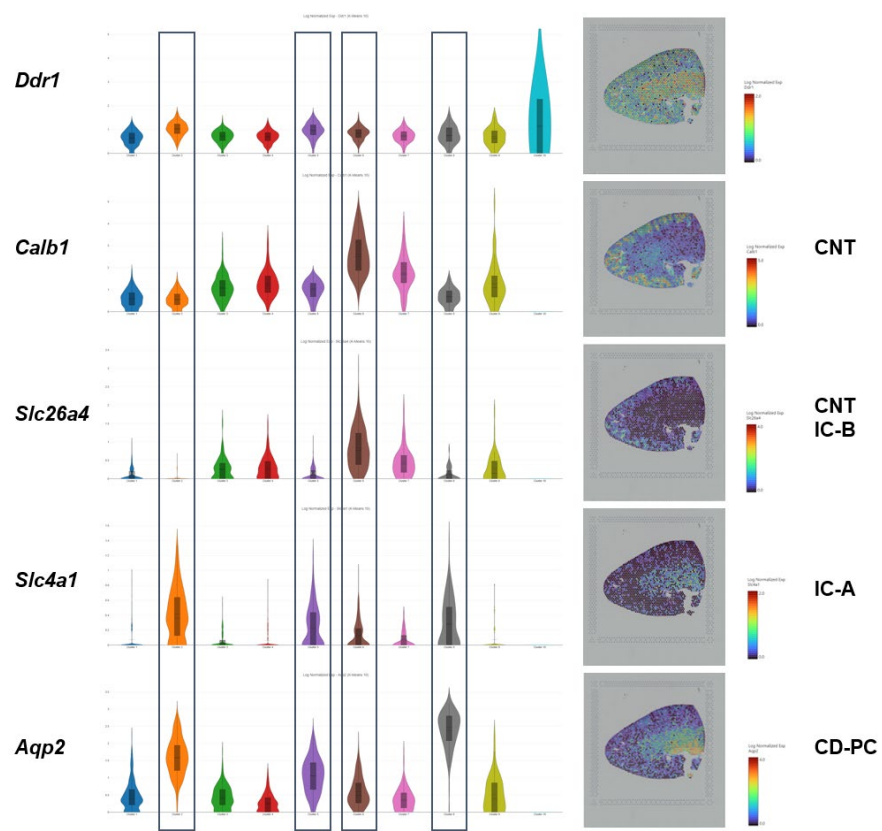
Research Division, Chugai Pharmaceutical Co., Ltd., Yokohama city, Kanagawa, Japan. (Y.Y., T.M., Y.T., N.H.)

Translational Research Division, Chugai Pharmaceutical Co., Ltd., Yokohama city, Kanagawa, Japan. (A.M.)

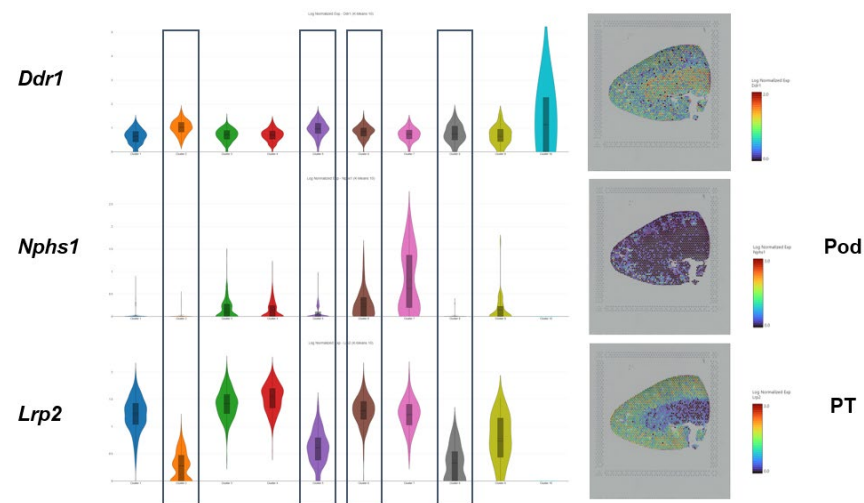
The Journal of Pharmacology and Experimental Therapeutics

JPET-AR-2024-002330

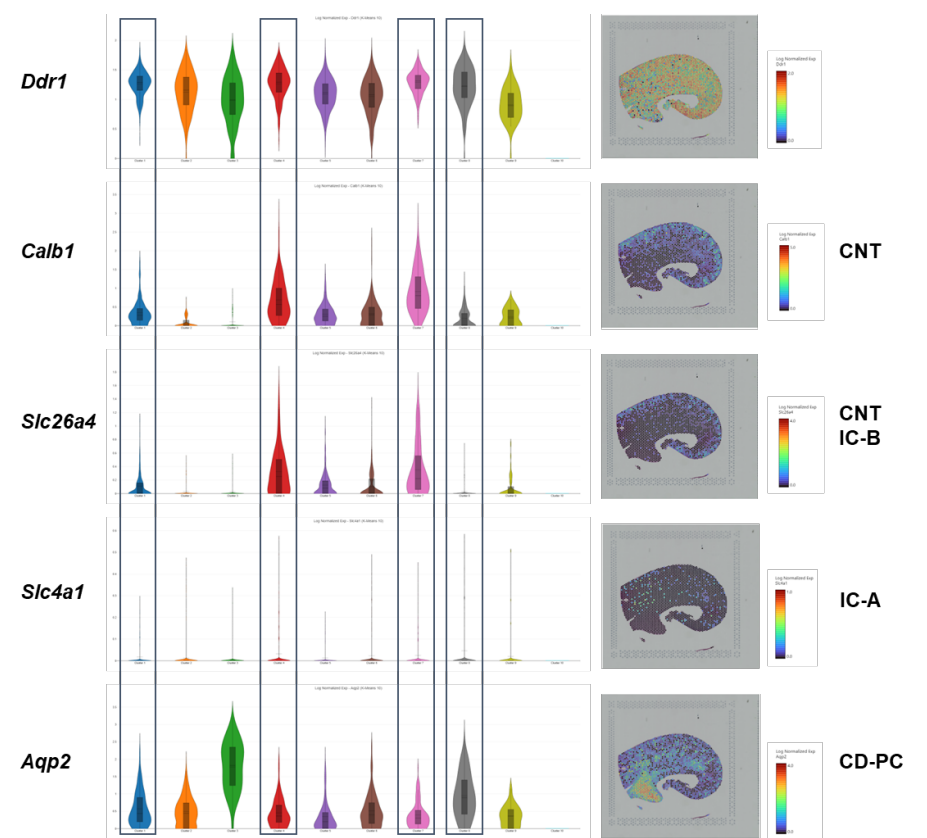
A



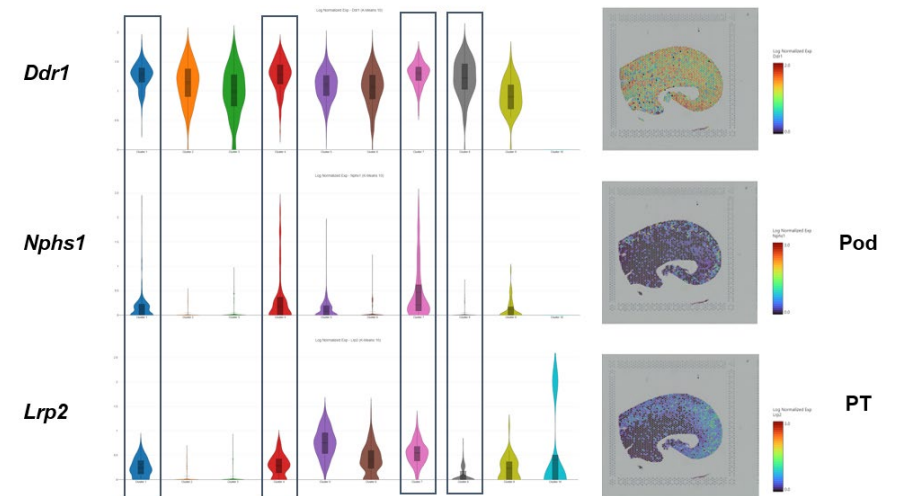
B



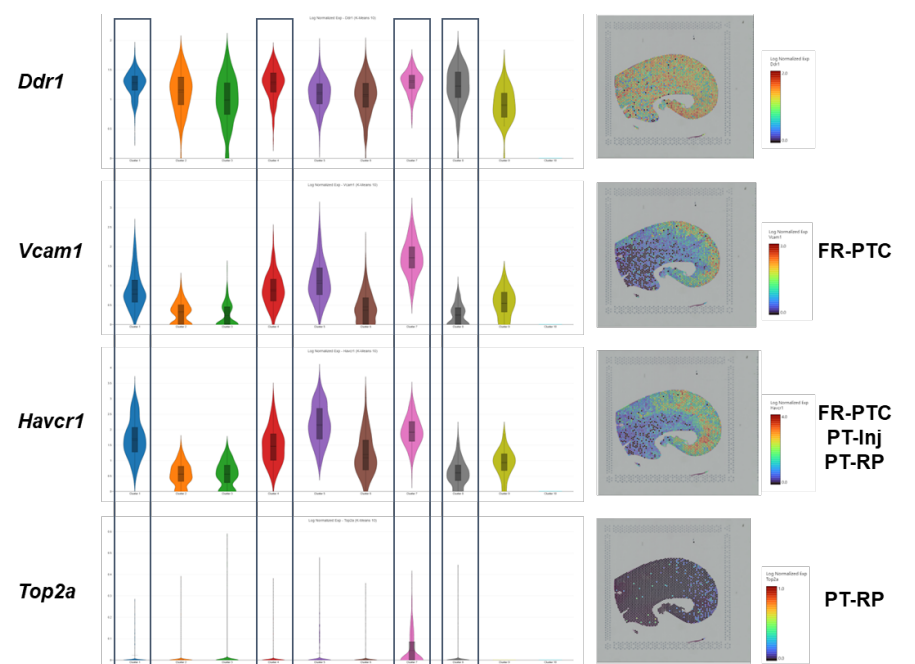
C



D



E



Supplemental Figure 3. Analysis of DDR1 expression spots in 10x Visium ST analysis. **(A-D)** Violin plot and localization of *Ddr1*, *Calb1*, *Slc26a4*, *Slc4a1*, *Aqp2*, *Nphs1*, and *Lrp2* mRNA expression in Sham **(A, B)** and UUO **(C, D)**. **(E)** Violin plot and localization of *Vcam1*, *Havcr1*, and *Top2a* mRNA expression in UUO. CNT, connecting tubule; CD-PC, principal cells of collecting duct; IC-A, type A intercalated cells of collecting duct; IC-B, type B intercalated cells of collecting duct; Pod, podocyte; PT, proximal tubule; PT-Inj, injured PT; PT-R, repairing PT; FR-PTC, failed repair PT cells.

CH6824025, potent and selective DDR1 inhibitor, reduces kidney fibrosis in UUO mice

Names of authors

Yukari Yasui, Takeshi Murata, Yoshinori Tsuboi, Atsuko Murai, Naoshi Horiba

Research Division, Chugai Pharmaceutical Co., Ltd., Yokohama city, Kanagawa, Japan. (Y.Y., T.M., Y.T., N.H.)

Translational Research Division, Chugai Pharmaceutical Co., Ltd., Yokohama city, Kanagawa, Japan. (A.M.)

The Journal of Pharmacology and Experimental Therapeutics

JPET-AR-2024-002330

A

GeneID	LOG2FC Vehicle vs 200 mg/kg	pValue
Calb1	1.764552444	0.02956
Spp2	1.364416902	0.01270
Per2	1.255077133	0.01166
Ptger3	1.249489811	0.01359
Slc34a3	1.163660232	0.02909
Fabp3	1.117383053	0.00940
Cox7a1	1.094389761	0.02626
Gpx6	1.0906129	0.04028
Gatm	1.066429923	0.00334
Chrna4	1.03188503	0.01366
Sostdc1	1.027444663	0.01256
Uroc1	1.016474906	0.04532
Slc5a2	1.009688821	0.04148
Klk1	0.994004546	0.00838
Tmem37	0.991051478	0.00397
Mfsd4a	0.972221237	0.03756
Atp5g1	0.968455697	0.00021
Ptgfr	0.955415725	0.02937
Hsd3b2	0.954384659	0.01569
Slc16a5	0.869044858	0.01260
Ppp1r1a	0.85589983	0.03727
Hlf	0.842433709	0.03156
Nol3	0.838198112	0.01464
Kcnt1	0.829788613	0.02004
Scd1	0.82133441	0.01625
Hsd17b14	0.811519827	0.00543
Osgin1	0.806013066	0.00790
Alas1	0.757539189	0.02051
Snca	0.752360931	0.00086
Dpp7	0.748610262	0.03001
Prodh2	0.727940122	0.04699
Chchd10	0.72276081	0.01543
Alas2	0.722745443	0.00852
Ldlr	0.720974324	0.03299
Rap1gap2	0.720451573	0.02600
Ftl1-ps1	0.718916136	0.00356
Tmed6	0.70819408	0.01497
Slc2a2	0.703306279	0.03960
Rph3a	0.699960354	0.04314
Fxyd2	0.699115684	0.01042
Car15	0.697617394	0.04554
Bpnt1	0.695528017	0.03750
Got1	0.684223222	0.02791
Isoc2a	0.678001134	0.01670
1700028J19Rik	0.676350656	0.04060
Atp5f1	0.667588993	0.01876
Tmem151a	0.665239083	0.01021
Gcat	0.655094282	0.03327
Hmgcr	0.651867221	0.02542
Pim3	0.643913208	0.01778

B

GeneID	LOG2FC Vehicle vs 200 mg/kg	pValue
Igfbp2	-3.17134207	3.488E-05
Dio2	-2.450456695	0.0030
Fbn2	-1.829747519	0.0001
Fcgbp	-1.627690547	0.0130
Mgl2	-1.442958852	0.0007
Apcdd1	-1.349505294	0.0009
Bcl6	-1.334579408	0.0487
Fndc1	-1.320896234	0.0060
Alx1	-1.276170555	0.0049
Sbspon	-1.241036667	0.0059
Spock3	-1.231780171	0.0476
Glipr2	-1.217840221	0.0196
Mxra8	-1.212318911	0.0064
Htr2b	-1.178151155	0.0096
Cd209a	-1.173934641	0.0215
Nrep	-1.172618184	0.0040
Ros1	-1.167875261	0.0058
Tnfrsf19	-1.166948062	0.0003
Tagln	-1.165167672	0.0277
Ptgs2	-1.135560301	0.0003
Wnt4	-1.132036472	0.0091
Cdh11	-1.11142357	0.0064
Ccr2	-1.100304181	0.0180
Crlf1	-1.092599379	0.0163
Pde2a	-1.088508423	0.0019
Aox3	-1.058711326	0.0038
Trp53i11	-1.039006581	0.0021
Oasl2	-1.025925366	0.0014
Plat	-1.0250561	0.0109
Robo3	-1.013306687	0.0037
Col3a1	-1.012825273	0.0139
Rnase6	-1.007173894	0.0020
Ramp1	-1.004878438	0.0113
Ltbp2	-0.994300976	0.0071
Mmd	-0.982140361	0.0012
Inhbb	-0.97678125	0.0220
Ptn	-0.964845054	0.0060
Vgll3	-0.950470258	0.0084
Gjb5	-0.94665546	0.0007
Col5a3	-0.945402892	0.0060
Ncam1	-0.940795371	0.0137
Npy1r	-0.935284215	0.0474
Cpxm1	-0.934721727	0.0172
Cd209c	-0.930119884	0.0008
Ccl17	-0.912418538	0.0007
Hs6st2	-0.900437103	0.0202
Dpt	-0.887814534	0.0440
Adgra1	-0.883176967	0.0181
Prss35	-0.882008285	0.0006
Adamts12	-0.881115849	0.0167

Supplemental Table 1. The list of the top 50 upregulated genes (**A**) and the top 50 downregulated genes (**B**) in CH6824025 group compared to Vehicle.